Soil Science
Issue: Volume 163(6), June 1998, pp 436-453

Publication Type: [Technical Articles]
ISSN: 0038-075X
Accession: 00010694-199806000-00002
Keywords: Soil hydraulic properties, parameter estimation, cone penetration testing, unsaturated hydraulic conductivity, inverse modeling

[Technical Articles]

ESTIMATING SOIL HYDRAULIC PROPERTIES FROM TRANSIENT CONE PERMEAMETER DATA

Kodešová, Radka[1]; Gribb, Molly M.[1]; Šimunek, Jirí[2]

Author Information

[1]Department of Civil and Environmental Engineering, University of South Carolina, 300 Main St., Columbia, SC 29208. Dr. Gribb is corresponding author. E-mail: gribb@sc.edu

[2]US Salinity Laboratory, USDA-ARS, 450 W. Big Springs Road, Riverside, CA 92507.
Received Oct 15, 1997; accepted Jan. 23, 1998.

Abstract

We present here a method for determining the hydraulic properties of unsaturated soil via inverse modeling. A modified cone penetrometer, called a cone permeameter, has been designed to inject water into the soil through a screen and to measure the progress of the wetting front with two tensiometer rings positioned above the screen. Cumulative inflow and pressure head readings are analyzed to obtain estimates of the hydraulic parameters describing the hydraulic conductivity curve $K(h)$ and the soil-moisture characteristic curve, [theta](h). Two sets of cone permeameter tests, which differ in the method of placement in the soil, are discussed. In the first case, the cone permeameter was buried; in the second case, it was placed by direct push to the testing depth. Optimizations for various sets of unknown parameters, with and without additional soil moisture information, were performed. The effects of applied pressure head at the source and of initial pressure readings on the resulting hydraulic parameters are investigated. The optimization results are compared with the results of standard laboratory and field methods. The saturated hydraulic conductivity was well estimated. For cases in which the saturated moisture content was estimated or fixed near the laboratory-derived value, the soil-moisture characteristic curves were between the wetting and drying curves obtained from other standard methods.

In the past, solution of variably saturated flow problems required use of analytical or quasianalytical equations and adherence to strict boundary and initial conditions. Today a wide variety of saturated-unsaturated flow codes exists for the numerical solution of such problems. Use of these codes, however, requires inputs of soil hydraulic properties. As a result, accurate descriptions of the soil-moisture characteristic and hydraulic conductivity curves, [theta](h) and $K(h)$, are particularly important. Although these soil properties can be determined in the laboratory, in situ methods that better reflect field behavior are often preferred.

In situ direct measurement of point data on the soil-moisture characteristic curve, [theta](*h*), and/or the hydraulic conductivity curve, *K*(*h*), may be obtained using a number of methods, including the instantaneous profile, crust, and infiltrometer methods (Klute and Dirksen 1986; Benson and Gribb 1997). Although the concept is relatively simple, these direct measurement methods have a number of limitations that restrict their use in practice. For example, most methods are very time consuming. Methods requiring repeated steady-state flow situations or other equilibrium conditions are also tedious, whereas linearizations and other approximations or interpolations to allow analytic or semianalytic inversions of the flow equation introduce additional errors. Finally, information about the uncertainty in the estimated hydraulic parameters is not readily obtained using direct inversion methods.

Parameter optimization is an indirect approach that makes it possible to obtain *K*(*h*) and [theta](*h*) simultaneously from transient flow data (Kool et al. 1987). In this case, a flow event is modeled with an appropriate governing equation and analytical expressions of *K*(*h*) and [theta](*h*). The unknown parameters of *K*(*h*) and [theta](*h*) are obtained by minimization of an objective function describing the differences between some measured flow variables and those simulated with a numerical flow code. This methodology was applied originally to laboratory one-step column outflow data (Kool et al. 1985; Parker et al. 1985; van Dam et al. 1992). To reduce the problem of nonuniqueness of the optimized parameters (Carrera and Neuman 1986), Toorman et al. (1992) investigated the use of pressure head data in addition to one-step outflow data. van Dam et al. (1994) showed that the transient outflow data alone obtained from a modified multistep column outflow experiment are sufficient to obtain unique estimates of the soil hydraulic properties. Finally Eching and Hopmans (1993) and Eching et al. (1994) presented an improved parameter estimation technique based on analysis of multi-step outflow volume and pressure head data. Parameter estimation has also been used with data obtained with the evaporation method described by Wind (1968) (see, for example, Santini et al. (1995); Ciollaro and Romano (1995); Šimunek et al. (1998a)). In this case, the upper boundary flux calculated from the decrease of weight of the soil sample with time is used as the upper boundary condition. Transient pressure head data from at least one location in a soil core and the total water volume at an arbitrary time (usually at the beginning or end of the experiment) are included in the formulation of the objective function. All of these laboratory methods provide information about the drying branches of the soil-moisture characteristics.

For field determination of the wetting branches of the soil hydraulic properties, Russo et al. (1991) and Bohne et al. (1993) studied the application of parameter estimation methods to ponded infiltration flow data. Šimunek and van Genuchten (1996) analyzed hypothetical tension disc infiltrometer flow data and showed that additional pressure head data are necessary for numerical convergence and uniqueness of the optimized parameters. As with one-step and multi-step column outflow experiments, they found later that only inflow data obtained from a multiple tension disc infiltrometer experiment with additional initial and final moisture contents from below the disc are sufficient to obtain unique estimates of the soil hydraulic properties (Šimunek and van Genuchten 1997). Another technique for gaining information about the drying branches of the soil hydraulic properties via multi-step soil water extraction and parameter optimization was developed by Inoue et al. (1998). They extracted water with a ceramic soil solution sampler at sequentially applied underpressure (vacuum) steps and analyzed cumulative extraction volume data along with pressure heads measured with tensiometers at three distances from the sampler.

The field methods described above are applicable only in the near surface. Gribb (1993, 1996) proposed a new cone penetrometer tool, a cone permeameter, and use of parameter optimization to estimate soil hydraulic properties at depth. A prototype cone permeameter was developed further by Leonard (1997) (Figs. 1 and 2). A detailed description of the prototype, its use under saturated and unsaturated conditions, as well as the typical courses of such experiments were presented by Gribb et al. (1998). For each test, the cone permeameter is placed in the soil, and a constant head is then applied to the 5-cm-long screen. Cumulative inflow volume is determined from scale readings of the mass of water removed from the source. Progress of the wetting front is measured with tensiometer rings 5 and 9 cm above the screen. After the water supply valve is closed, the tensiometers monitor the redistribution of water in the soil profile.

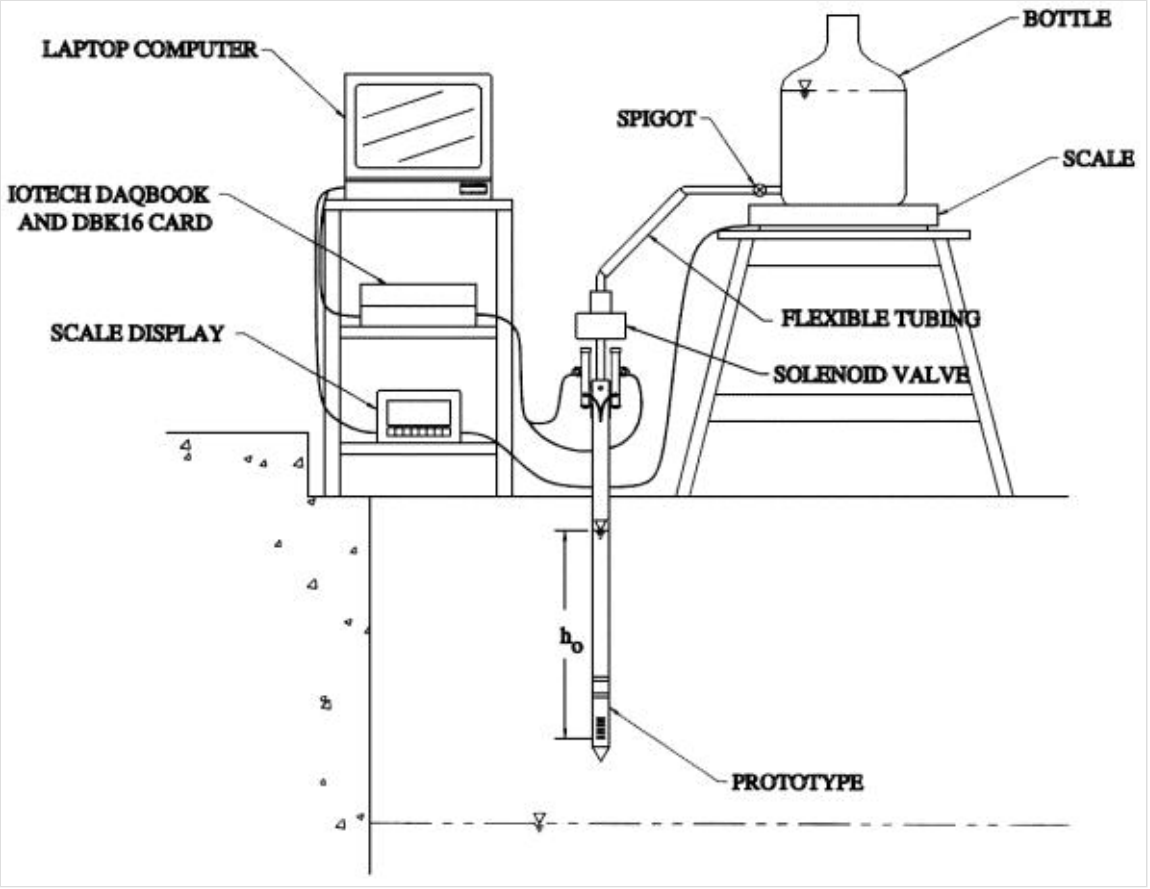

Fig. 1. Cone permeameter test set up.

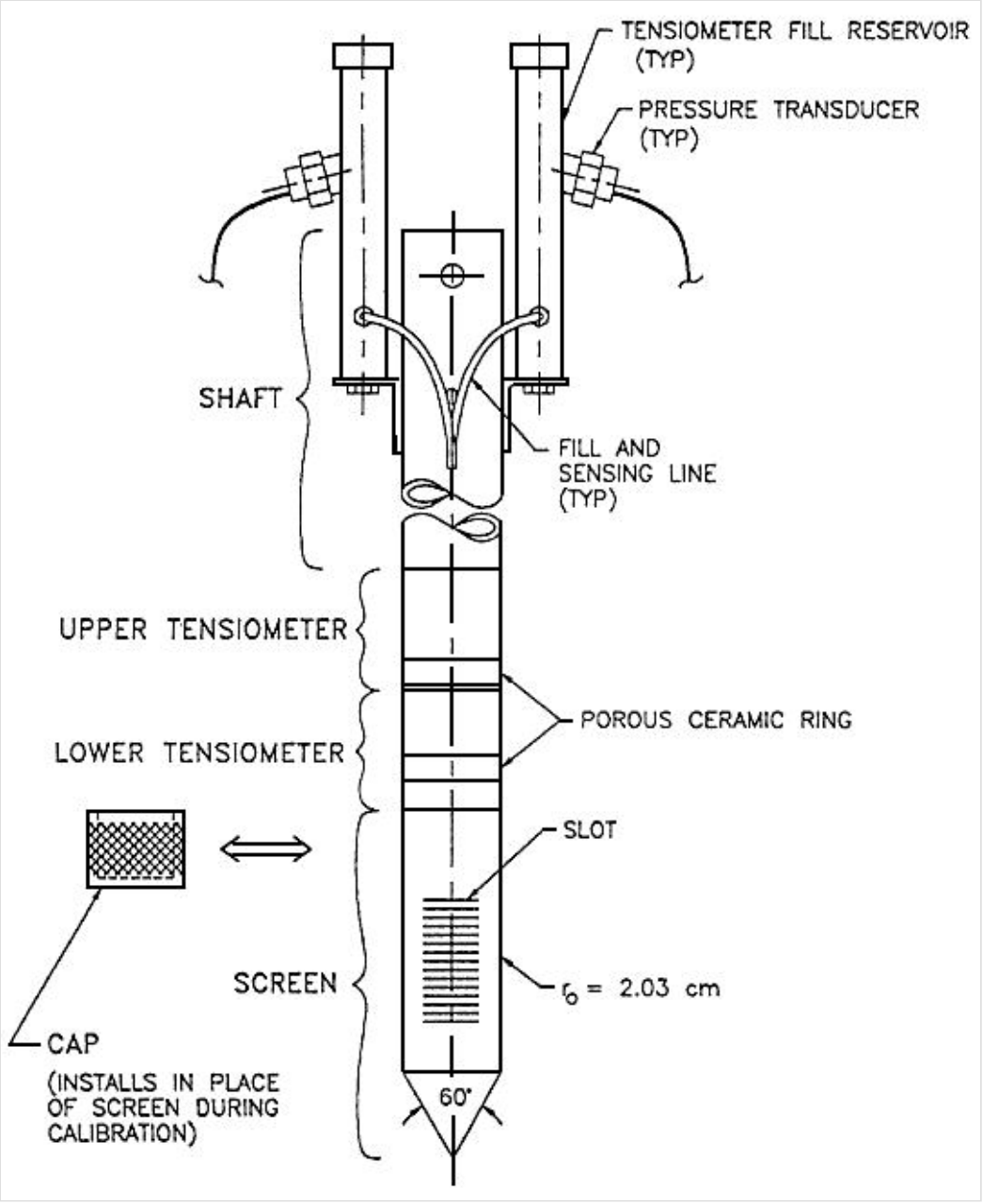

Fig. 2. Prototype cone permeameter.

Here we present observed data and numerical analysis of data collected during the wetting periods of tests performed by Leonard (1997) in a laboratory aquifer system. The numerical inverse code of Šimunek and van Genuchten (1996) was used to predict the soil hydraulic properties of the tested soil from cumulative inflow volume and pressure head data. It is obvious that the way in which the cone permeameter is placed in the soil can influence the hydraulic property values determined by parameter optimization. To study this issue, we selected two sets of tests. The first set of tests was performed with the permeameter after it was buried in the soil, and a second set of tests was conducted after direct push to the testing depth. Next, we investigated the impact of different applied pressure heads and initial conditions on the courses of the experiments and, consequently, the parameter estimates for both sets of tests. Gribb (1996) showed that inverse analysis of data obtained with the cone permeameter provides good estimates of K_s and [alpha] values, but that the method is less able to predict the real values of $[theta]_s$ and n (see Eqs. (4) and (5) below). Therefore, to improve parameter estimates, we included initial and final soil moisture data in the analysis, as recommended by Šimunek and van Genuchten (1997).

$$\theta_e = \frac{\theta(h) - \theta_r}{\theta_s - \theta_r} = \frac{1}{(1 + |\alpha h|^n)^m} \quad h < 0$$

$$\theta_e = 1, h \geq 0$$

Equation 4

$$K(\theta) = K_s \, \theta_e^l \left[1 - (1 - \theta_e^{1/m})^m\right]^2 \quad h < 0$$

$$K(\theta) = K_s \quad h \geq 0$$

Equation 5

THEORY

HYDRUS-2D (Šimunek et al. 1996) is used to simulate the cone permeameter test in unsaturated soil with the finite element mesh shown in Fig. 3. The governing flow equation for radially symmetric isothermal Darcian flow in an isotropic, rigid, porous medium, assuming that the air phase plays an insignificant role in the liquid flow process, is (Richards 1931): Equation (1) where *r* is the radial coordinate (L), *z* is the vertical coordinate positive upward (L), *t* is the time (T), *h* is the pore water pressure head (L), and K (L/t) and [theta] (L^3L^{-3}) are the hydraulic conductivity and volumetric moisture content, respectively. Equation (1) is solved numerically for the following boundary and initial conditions: Equations (2) and (3) where h_i is the initial pressure head in the soil (L), h_0 is the supply pressure head imposed at the bottom of the screen (L), z_0 is the coordinate of bottom of the screen (L), *L* is the length of the screen, and r_0 is the radius of the screen (L). Exterior boundaries are located far enough from the source that they do not to influence the solution and are defined as no-flow boundaries.

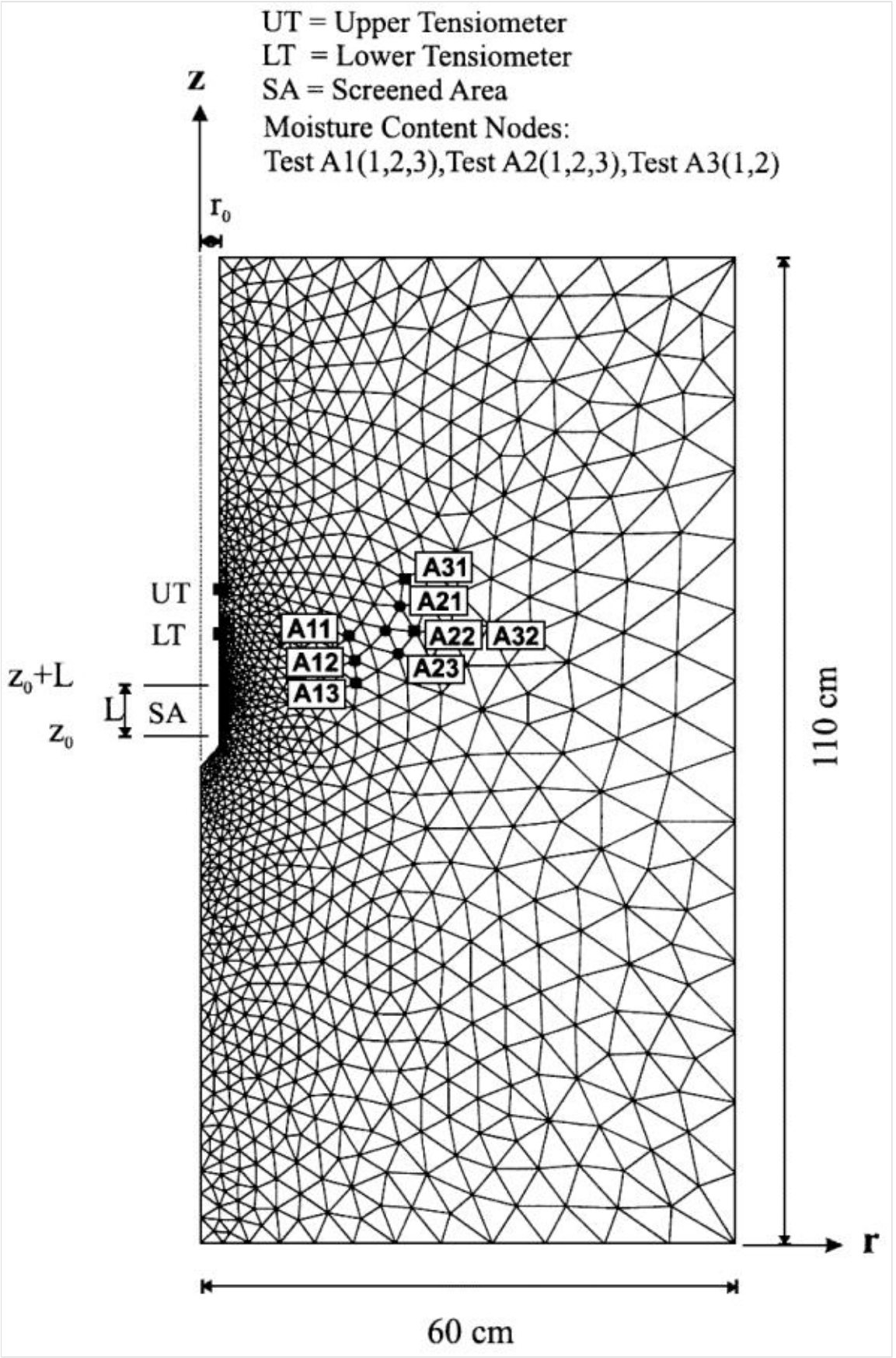

Fig. 3. Finite element mesh used for modeling cone permeameter test and location of moisture content samples.

$$\frac{1}{r}\frac{\partial}{\partial r}\left[r\,K\frac{\partial h}{\partial r}\right]+\frac{\partial}{\partial z}\left[K\left(\frac{\partial h}{\partial z}+1\right)\right]=\frac{\partial\theta}{\partial t}$$

Equation 1

$$h\,(r,z,t)=h_i\,(r,z)\qquad t=0$$

Equation 2

$$h\,(r,z,t)=h_o-(z-z_o)\quad r=r_o,\ z_o<z<z_o+L$$

Equation 3

The van Genuchten (1980) expressions for moisture content and hydraulic conductivity, [theta](h) and K([theta]), are used in this work: Equations (4) and (5) where $[\theta]_e$ is the effective water content (-), K_s is the saturated hydraulic conductivity (L/T), $[\theta]_r$ and $[\theta]_s$ are the residual and saturated water contents (L^3L^{-3}), respectively, l is the pore-connectivity parameter (-), and [alpha] (L^{-1}), n and m (= 1 - 1/n) are empirical parameters. The predictive K([theta]) model is based on the capillary theory of Mualem (1976) in conjunction with Eq. (4). The pore-connectivity parameter, l, in the hydraulic conductivity function was estimated by Mualem (1976) to be about 0.5 for many soils. The hydraulic characteristics defined by Eqs. (4) and (5) contain five unknown parameters: K_s, $[\theta]_r$, $[\theta]_s$, [alpha], and n.

The objective function, [PHI], minimized during the parameter optimization process, is (Šimunek et al. 1998b): Equation (6) where the first term on the right-hand side represents deviations between measured and predicted space-time variables (e.g., observed pressure heads or moisture contents at different locations and/or times, or the cumulative infiltration rate versus time). In this term, m_q is the number of different sets of measurements, and n_{qj} is the number of measurements in a particular measurement set. The q * [over] j (x,t_i) terms represent specific measurements at time t_i for the jth measurement set at location x(r,z), q_j($x,t_i,\boldsymbol{b}$) are the corresponding model predictions for the vector of optimized parameters $\boldsymbol{b}$ (e.g., $[\theta]_r$, $[\theta]_s$, [alpha], n, and K_s), and v_j and $w_{i,j}$ are weights associated with a particular measurement set or point, respectively. The weighting factor, v_j, is given by the inverse of the number of measurements multiplied by the variance of those observations, and $w_{i,j}$ is equal to 1 in this case. The second term of Eq. (6) represents differences between independently measured and predicted soil hydraulic properties (e.g., soil-moisture characteristic, [theta](h), hydraulic conductivity, K([theta]) or K(h), and/or diffusivity, D([theta]) or D(h) data), whereas the terms m_p, n_{pj}, p * [over] j ($[\theta]_i$), p_j($[\theta]_i,\boldsymbol{b}$), $\bar{v}_j$ and $\bar{w}_{i,j}$ have meanings similar to those in the first term but now stand for the soil hydraulic properties. The last term of Eq. (6) represents a penalty function for deviations between prior knowledge of the soil hydraulic parameters, b * [over] j, and their final estimates, b_j, where n_b is the number of previously known parameters and v_j are their preassigned weights. Estimates made with prior information (such as those used in the third term of Eq. (6)) are known as Bayesian estimates (Bard 1974). Note that the covariance (weighting) matrices that provide information about the measurement accuracy, as well as any possible correlation between measurement errors and/or parameters, are assumed to be diagonal in this study.

$$\Phi(b, q, p) = \sum_{j=1}^{m_q} v_j \sum_{i=1}^{n_{qj}} w_{i,j} \left[q^*_j (x, t_i) - q_j (x, t_i, b) \right]^2 + \sum_{j=1}^{m_p} v_j \sum_{i=1}^{n_{pj}} w_{i,j} \left[p^*_j (\theta_i) - p_j (\theta_i, b) \right]^2 + \sum_{j=1}^{n_b} \hat{v}_j \left[b^*_j - b_j \right]^2$$

Equation 6

Minimization of the objective function [PHI] is accomplished by using the Levenberg-Marquardt nonlinear minimization method (Marquardt 1963), which combines the Newton and steepest descent methods.

METHODS

The Laboratory Aquifer

Prototype tests were conducted in a laboratory aquifer measuring 4.7 m × 4.7 m × 2.6 m. The aquifer material is a sandy soil with occasional kaolin pockets and is underlain by 20 cm of gravel. The average bulk density of undisturbed soil samples was determined to be 1.69 g/cm^3. A description of the aquifer and its soil properties was presented previously by Gribb et al. (1998). To simulate field conditions with various soil moisture profiles, the water table in the laboratory aquifer was raised and/or lowered by pumping water in/out of a French drain system. The hydraulic properties of the soil were determined directly using several standard methods. Pressure plate (ASTM D-2434) capillary rise (Lambe 1951) and computer-automated extraction/sorption (Ray and Morris 1994) tests were performed to evaluate the drying and wetting branches of the retention curve, respectively (Singleton 1997). The nonlinear optimization program, RETC, (van Genuchten et al. 1991) was used to fit [theta](h) data to Eq. (4). Constant head permeability tests (ASTM D-2334) were performed in the lab, and slug (Bouwer and Rice 1976) and Guelph permeameter (Reynolds 1993) tests were performed in situ to determine K_s (Scaturo 1993; Singleton 1997).

Test Procedure

Two sets of cone permeameter tests were performed by Leonard (1997). In the first case (Set A), the prototype was placed in a hole and the soil carefully backfilled around it (12/20/96). In the second case (Set B), the cone permeameter was pushed continuously to the testing depth by a drill rig (01/28/97). These two sets of tests and results obtained via inverse modeling demonstrate the effects of placement on the optimized hydraulic properties of the soil.

The Set A tests were conducted with the cone permeameter after it was buried in the soil. The center of the screened section was 65 cm below the soil surface. The water table was raised to the soil surface and then drawn down 26 and 48 cm below ground surface before testing. Under these saturated conditions, the prototype was used as a piezometer, and Hvorslev's (1951) simple analytical equation was used to obtain saturated hydraulic conductivity values. The detailed test procedure and data analysis were described by Leonard (1997) and Gribb et al. (1998). The water table was then lowered to approximately 190 cm below the soil surface, and the laboratory aquifer was not disturbed for 2 weeks, after which time several tests were run under unsaturated conditions. This depth and length of time ensured that the tests would not be influenced by the water table and that low initial pressure heads would be detected by the tensiometers. Sufficiently low initial pressure heads were important so that a wide range of pressure heads would be monitored during a test and the corresponding moisture content range during data collection would be large enough to minimize nonuniqueness problems. It is necessary at this point to note that the initial pressure heads measured with both tensiometers were always higher than -50 cm for all of the tests we conducted in the laboratory aquifer because it was not possible to induce lower heads. It is evident from our experience with this soil that the equivalent moisture content at this pressure head level is close to $[theta]_r$, and the corresponding low hydraulic conductivities constrain moisture redistribution in the laboratory aquifer. Similar circumstances were also discussed by Inoue et al. (1998). In their numerical simulations of soil water extraction experiments in sandy soil, pressure heads did not decrease below -35 cm, again because of the limiting function of low hydraulic conductivities near $[theta]_r$.

Three representative tests were selected to demonstrate the influence of different applied pressure heads and variable initial pressure head readings on the course of the experiment and, finally, on the inverse solution results. A summary of the applied boundary condition and the observed initial and final conditions is shown in Table 1. Flow data were collected electronically every second for $0 < t < 840$ s (Leonard 1997; Gribb et al. 1998). A water pressure head of 50 cm was supplied to the center of the screen for $0 < t < 400$ s for the test performed on 01/06/97 (Test A1), and a water pressure head of 30 cm was applied for $0 > t > 440$ s for the tests conducted on 01/25/97 (Test A2) and 01/26/97 (Test A3). After the source of water was terminated, data collection continued as the water redistributed in the flow regime. Only inflow and pressure head data obtained at 5-s intervals for $0 < t < 400$ s were used to obtain wetting branches of the soil hydraulic characteristics with the parameter estimation procedure.

Test	Date	Applied pressure head (cm)	Initial pressure head readings (cm)		Final pressure head readings (cm)		Final cumulative infiltration volume (cm^3)
			Lower tensiometer	Upper tensiometer	Lower tensiometer	Upper tensiometer	
A1	01/06/97	52.5	−47.6	−50.2	−8.9	−15.9	11217
A2	01/25/97	32.5	−47.4	−49.3	−11.3	−18.3	6368
A3	01/26/97	32.5	−30.2	−31.5	−13.0	−20.0	5438
B1	01/30/97	32.5	−45.1	−48.4	−12.8	−22.3	2222
B2	01/31/97	52.5	−45.0	−46.7	−10.8	−18.0	5438

TABLE 1 Applied boundary conditions and observed initial and final conditions for Set A and B tests

The second set of tests (Set B) was conducted with the prototype after it was pushed into the soil to a depth of 70 cm. In this case, tests were run under unsaturated conditions immediately after placement of the prototype. Two representative tests run with the same applied water pressure heads as used for Set A are shown here to demonstrate again the influence of different applied boundary conditions (Table 1). However, in the case of Set B, we chose tests performed in the reverse order to illustrate that the soil hydraulic properties changes attributed to the applied pressure head differences in Set A (see Discussion) were not attributable to repetition of experiments in the same location. As with the previous set of tests, flow data were electronically collected every second for $0 < t < 840$ s (Leonard 1997). A water pressure head of 30 cm was supplied to the center of the screen for $0 < t < 540$ s for the test performed on 01/30/97 (Test B1), and a water pressure head 50 cm was supplied for $0 < t < 440$ s for the test conducted on 01/31/97 (Test B2). Pressure head and inflow data obtained at 5-s increments for $0 < t < 400$ s were used in the parameter estimation problem.

Inverse Solutions

Initial conditions for modeling were based on the pressure head conditions in the laboratory aquifer. For Set A, the water table was 189 cm, 183 cm, and 184 cm below ground surface for Tests A1, A2, and A3, respectively. However, the initial readings of the lower and upper tensiometers were as follows: Test A1: -47.6 cm and -50.2 cm; Test A2: -47.4 cm and -49.3 cm; and Test A3: -30.2 cm and -31.5 cm (Table 1). The volumetric moisture contents of soil samples taken at the same depth as the tensiometers were determined to be approximately 8% for all three tests. Because the soil moisture distribution was neither hydrostatic nor uniform before testing, the pressure heads in the domain were set equal to the upper tensiometer initial reading for elevations at or above that of the upper tensiometer. Similarly, the pressure heads at the elevation of the lower tensiometer or below were set equal to the lower tensiometer initial reading. The pressure heads between the two tensiometers were distributed linearly. The external boundaries were set as no-flow boundaries. The screen was modeled as a constant head boundary, with water pressure heads ranging from 52.5 to 47.5 cm (or 32.5 to 27.5 cm) from bottom to top for $0 < t < 400$ s. The water table was 183 cm and 184 cm below ground surface for Tests B1 and B2, respectively. In the case of Set B, initial readings of lower and upper tensiometers were as follows: Test B1: -45.1 cm and -48.4 cm; Test B2: -45.0 cm and -46.7 cm (Table 1). The soil moisture distribution was again neither hydrostatic nor uniform before testing, and, thus, the initial and boundary conditions were set up similarly to the previous examples.

Four inverse solutions for each test of Set A were obtained with different sets of parameters to be optimized and different inputs to the objective function. A summary of the solutions is shown in Table 2. In the first case, Inverse Solution 1 yielded estimates of the unknown parameters, [alpha], *n,* $[\theta]_s$ and K_s for $[\theta]_r = 0.008$ cm^3/cm^3. In the second case, Inverse Solution 2 yielded estimates of [alpha], *n,* and K_s for $[\theta]_s = 0.35$ cm^3/cm^3 and $[\theta]_r = 0.008$ cm^3/cm^3. In the third and fourth cases, additional moisture content information was introduced into the objective function to find a more realistic estimate of $[\theta]_s$. For Inverse Solution 3, the impact of a $[\theta](h)$ point given by the initial soil moisture content paired with the initial reading of the upper tensiometer was investigated using the second term of Eq. (6). Solely for Inverse Solution 4, the moisture contents of undisturbed soil samples taken at locations corresponding to nodes shown in Fig. 3, were determined at 400 s, 380 s, and 340 s for tests A1, A2, and A3, respectively, and this information was included in the first term of Eq. (6). Inverse Solutions 3 and 4 yielded estimates of the unknown parameters, [alpha], *n,* $[\theta]_s$ and K_s for $[\theta]_r = 0.008$ cm^3/cm^3. As a result of nonconvergence, we were unsuccessful in our attempts to obtain estimates of the unknown parameters when initial and final moisture content data were included in the objective function.

Inverse solution	Optimized parameters	Additional inputs
IS1	α, n, θ_s, K_s for $\theta_r = 0.008$	
IS2	α, n, K_s for $\theta_s = 0.35$ and $\theta_r = 0.008$	
IS3	α, n, θ_s, K_s for $\theta_r = 0.008$	Point of the retention curve $\theta(h)$
IS4	α, n, θ_s, K_s for $\theta_r = 0.008$	Soil moisture contents at different times and locations

TABLE 2 Summary of inverse solutions IS1-IS4 for Set A and Set B tests.

For Set B tests, soil moisture contents were not measured because of difficulties encountered while trying to sample the well consolidated soil. Therefore, we executed Inverse Solutions 1 and 2 on these data sets. In addition, because the initial tensiometer readings for tests B1 and B2 were similar to those for Set A, an initial soil moisture content of 8% was paired with the pressure head reading of upper tensiometer, and Inverse Solution 3 was also performed.

In all cases, the value of the residual moisture content was set equal to the value obtained from capillary rise experiments inasmuch as we anticipated that it would not be identifiable from the near-saturated tests. The first estimate of the optimized parameters had to be set within a realistic range of values characteristic for sandy soil to obtain reasonable final estimates. Use of extreme values for the initial estimates resulted in nonconvergence of the solution. The finite element mesh shown in Fig. 3 has been designed specifically for sandy soil. It should be noted that the mesh must be reconstructed for different soil types to ensure numerical stability of the solution.

RESULTS AND DISCUSSION

Comparison of Inverse Solutions

Results of the optimization processes and the representative hydraulic property values obtained using standard techniques are shown in Figs 4 through 12 and Tables 3, 4 through 5. Measured and simulated cumulative flow and pressure head data in time from the five inverse solutions are plotted in Figs 4-8. The estimated retention curves for all solutions of the five cone permeameter tests, along with those determined independently with capillary rise, the extraction/sorption, and pressure plate tests (Singleton 1997) are presented in Figs 9 through 12. Table 3 shows the hydraulic parameters [alpha], *n,* $[\theta]_s$ and K_s estimated via inverse modeling. Table 4 contains the hydraulic parameters [alpha], *n,* $[\theta]_r$ and $[\theta]_s$ of the retention curves obtained with standard laboratory methods. Finally, Table 5 presents the mean values of K_s determined with the cone permeameter under saturated conditions (Leonard 1997; Gribb et al. 1998), slug tests (Scaturo 1993), Guelph permeameter tests (Scaturo 1993; Singleton 1997), and laboratory constant head tests (Singleton 1997).

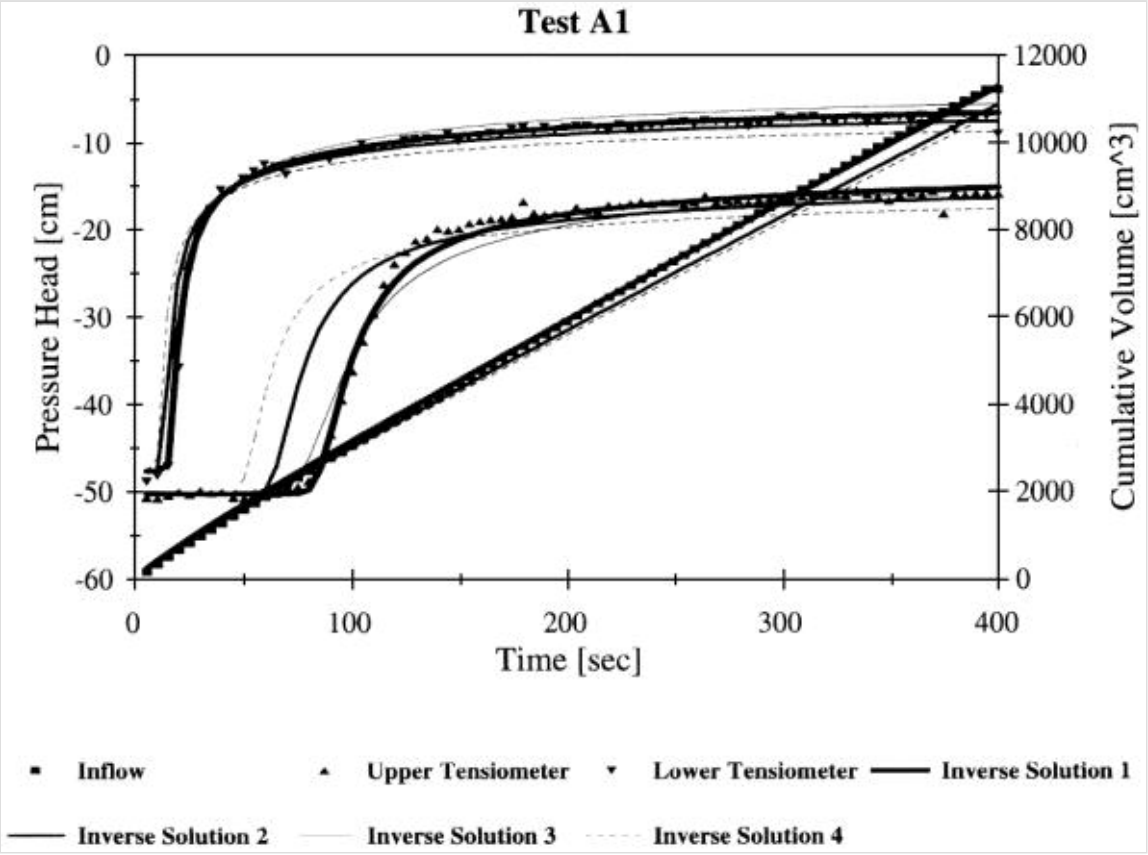

Fig. 4. Measured and simulated flow responses for Test A1.

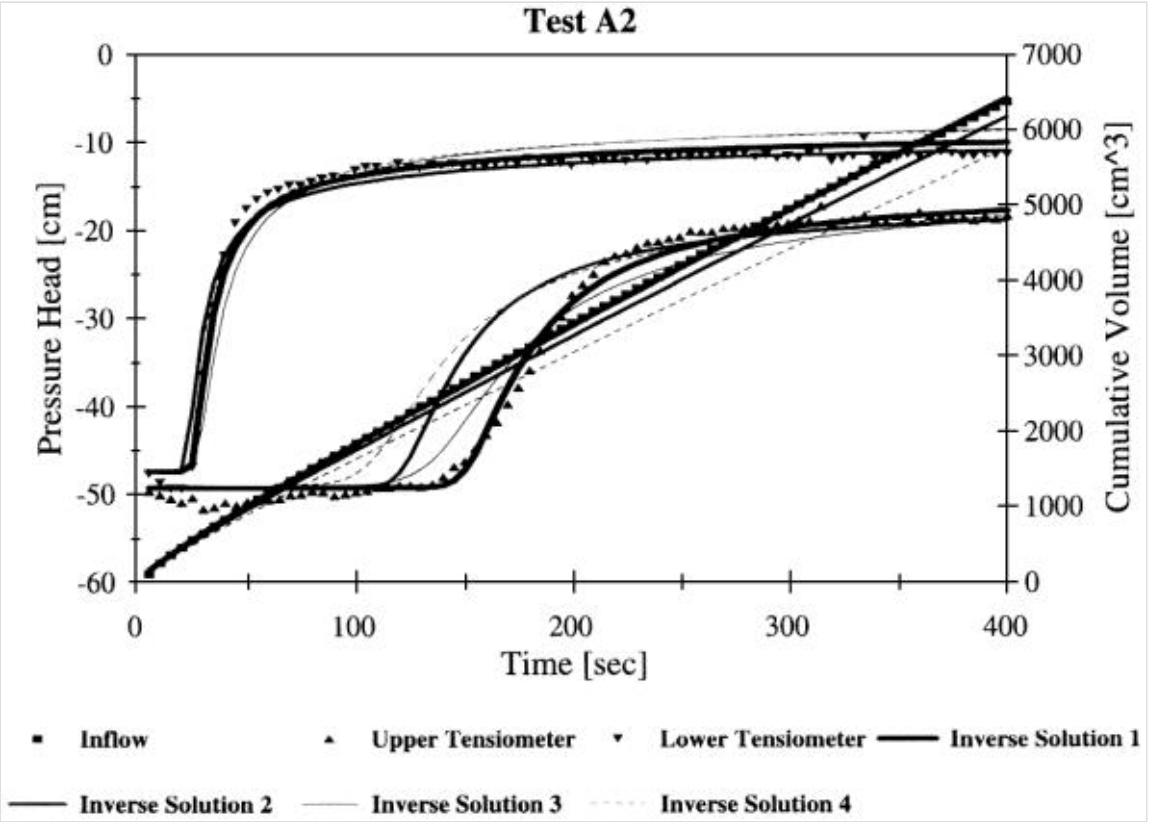

Fig. 5. Measured and simulated flow responses for Test A2.

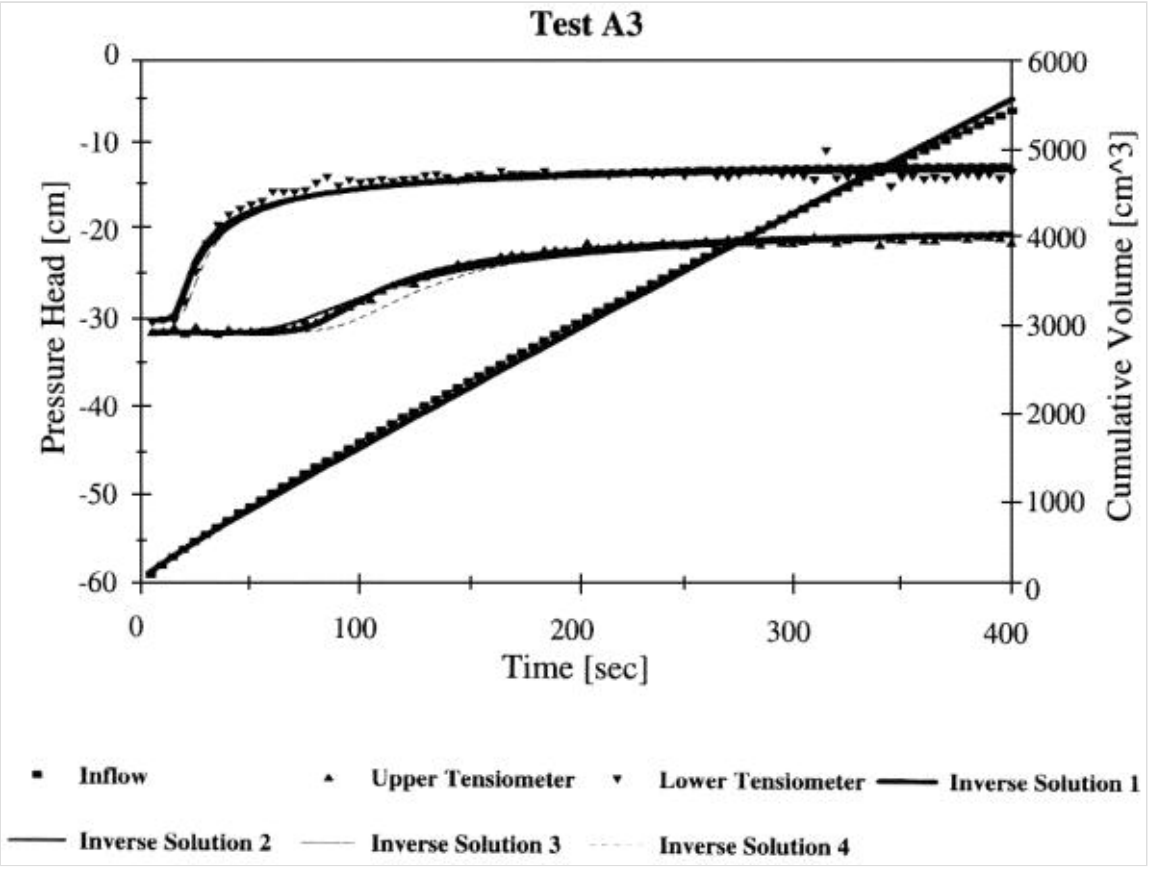

Fig. 6. Measured and simulated flow responses for Test A3.

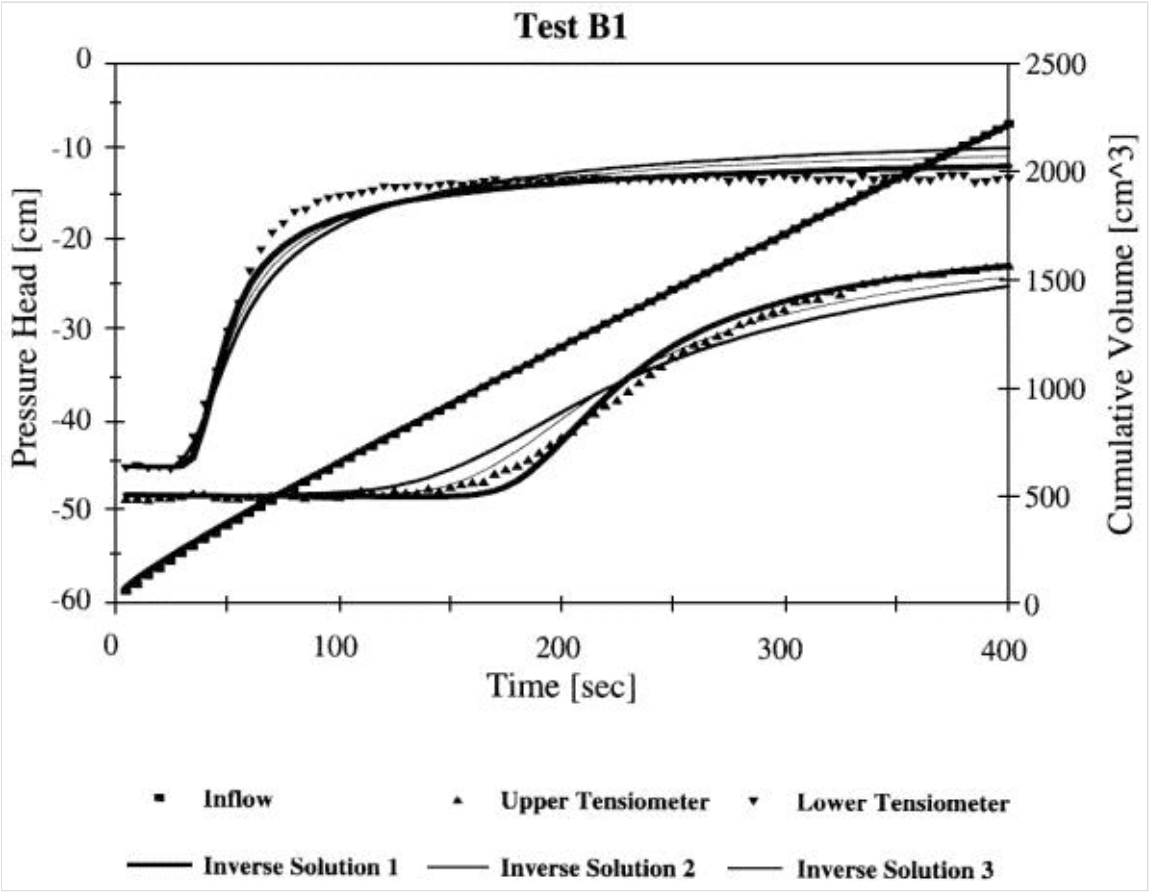

Fig. 7. Measured and simulated flow responses for Test B1.

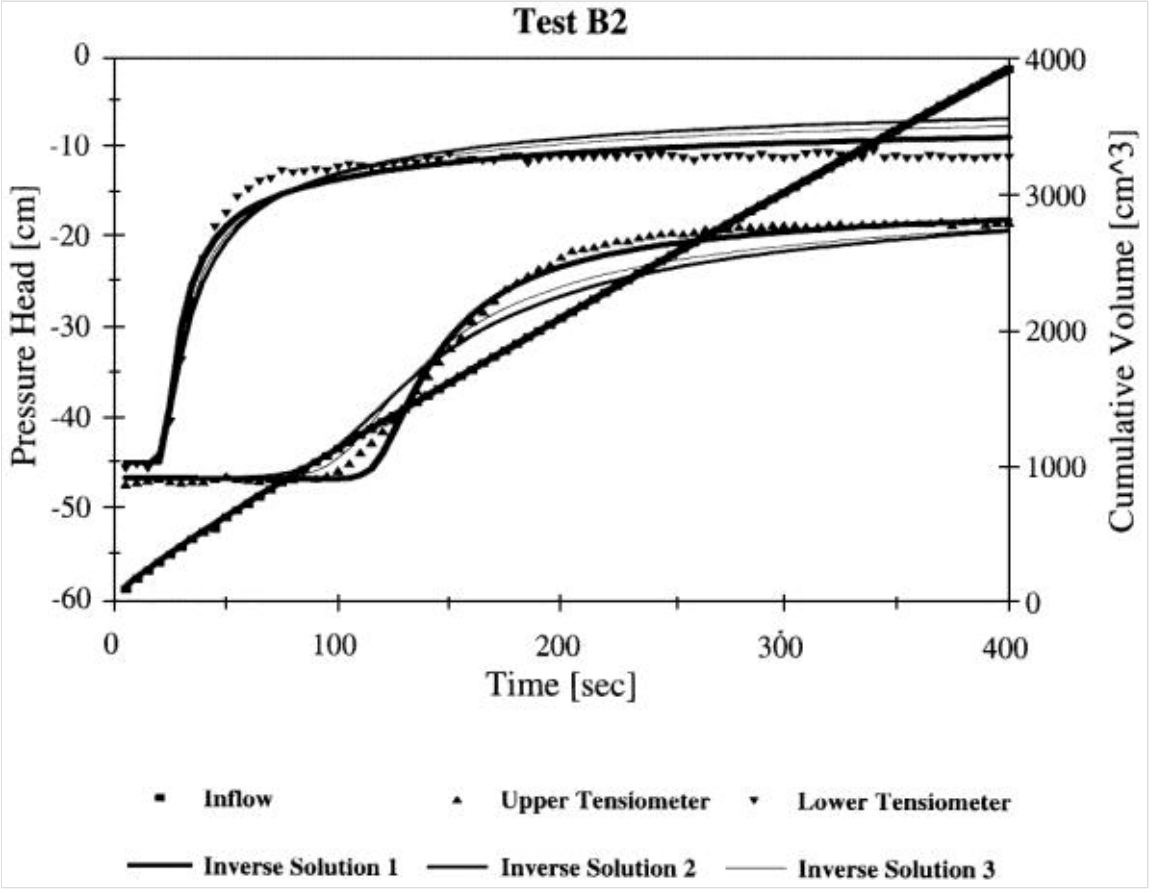

Fig. 8. Measured and simulated flow responses for Test B2.

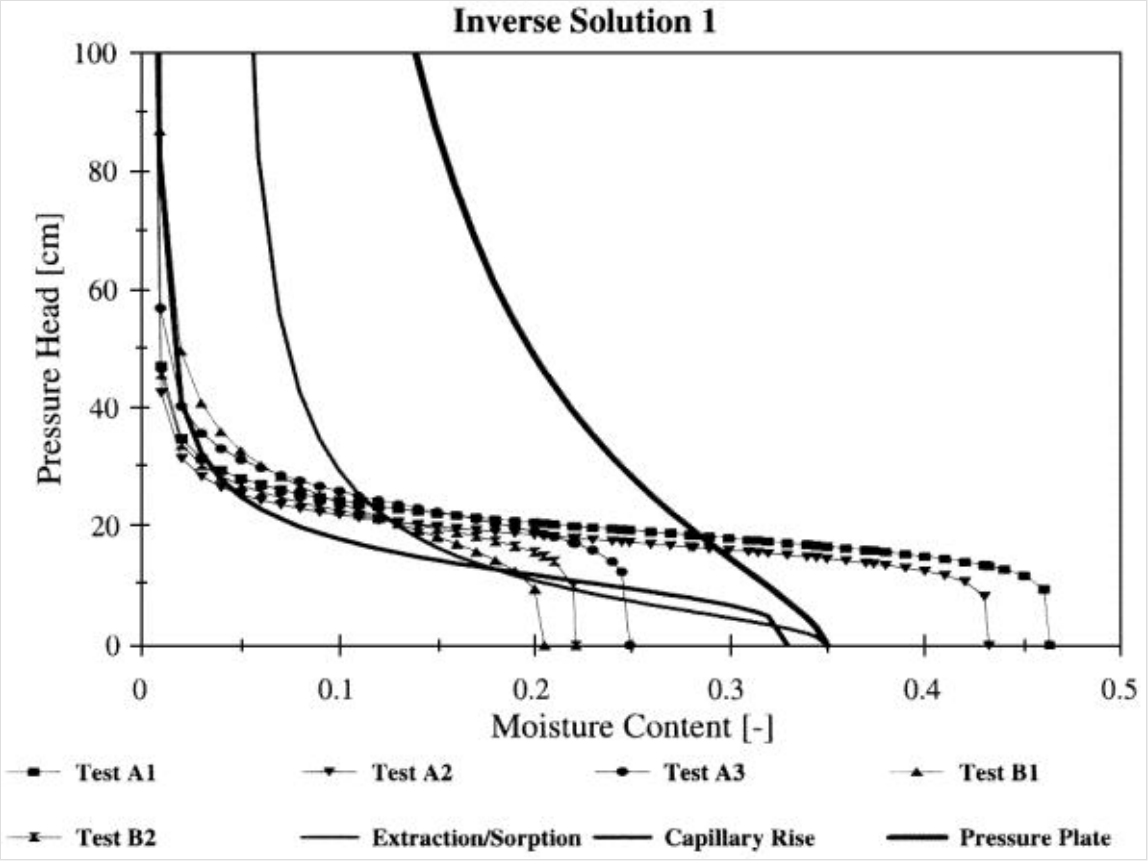

Fig. 9. Soil-moisture retention curves obtained with standard methods and those obtained from Inverse Solution 1 for Tests A1, A2, A3, B1, and B2.

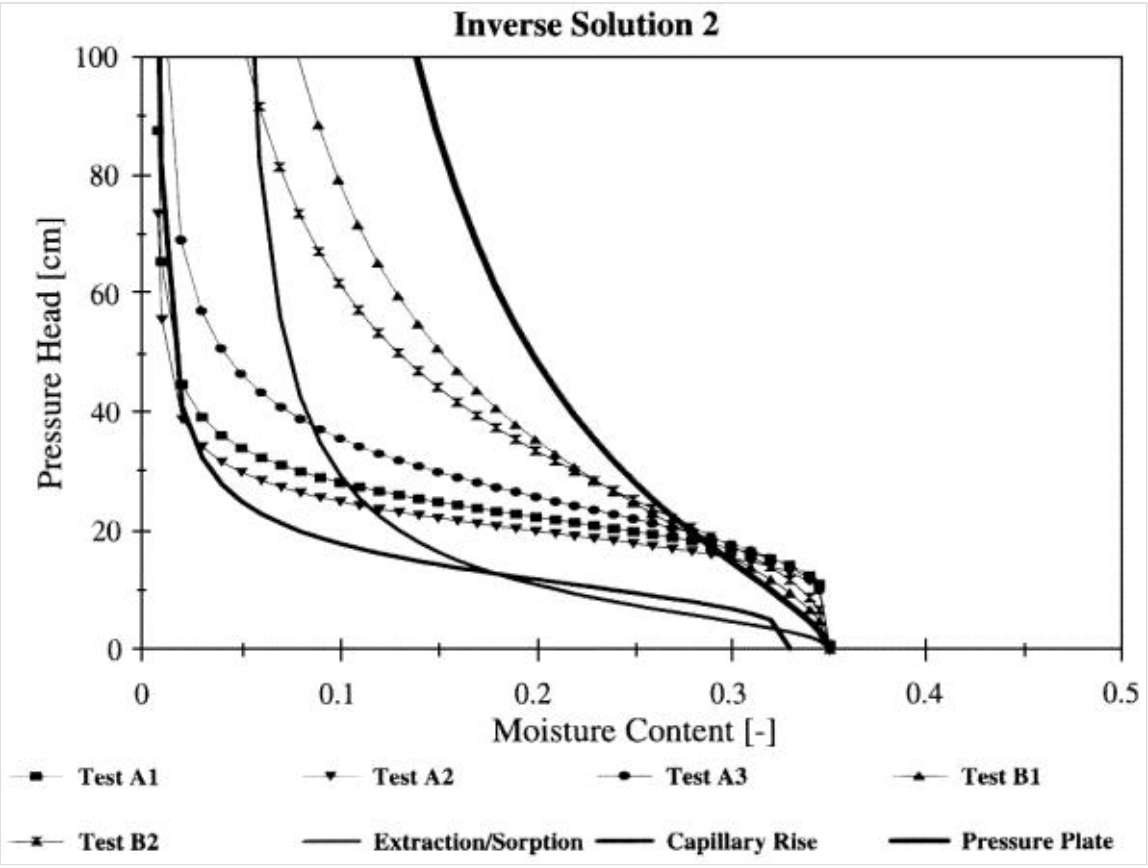

Fig. 10. Soil-moisture retention curves obtained with standard methods and those obtained from Inverse Solution 2 for Tests A1, A2, A3, B1, and B2.

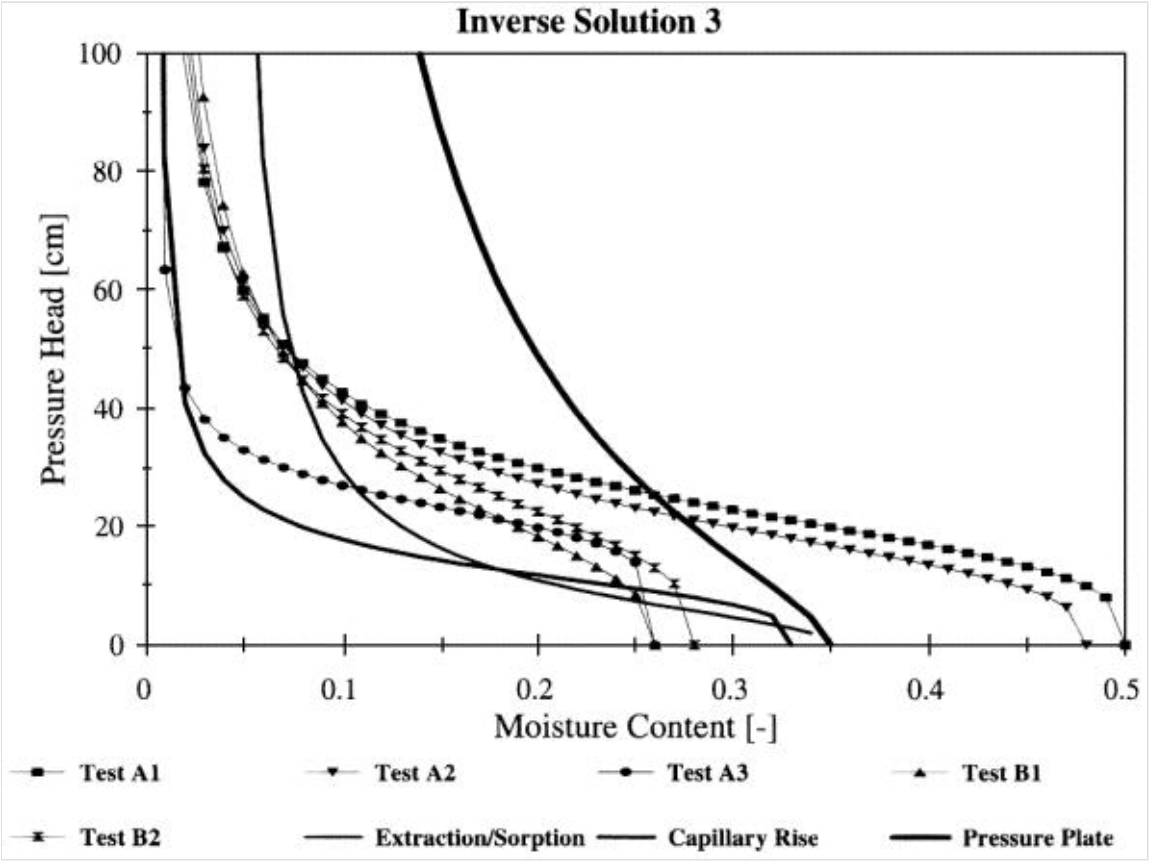

Fig. 11. Soil-moisture retention curves obtained with standard methods and those obtained from Inverse Solution 3 for Tests A1, A2, A3, B1, and B2.

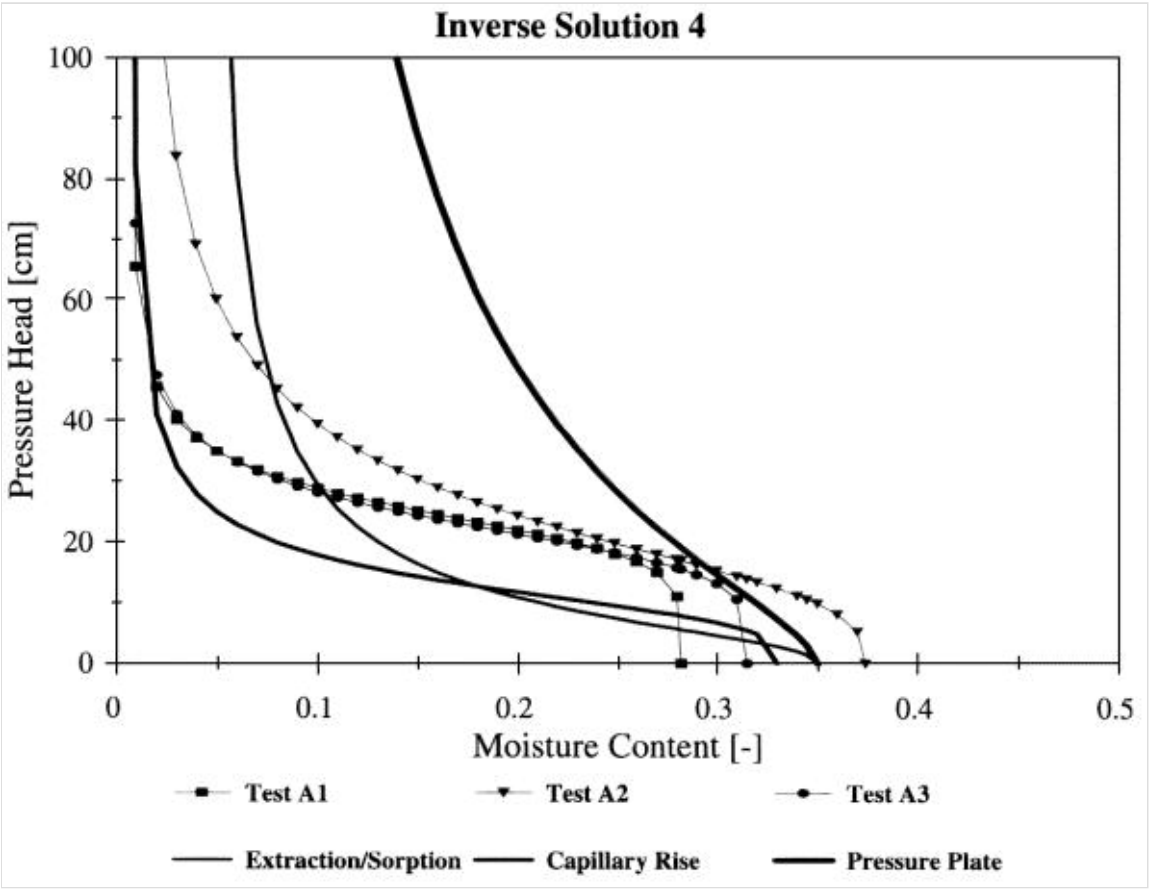

Fig. 12. Soil-moisture retention curves obtained with standard methods and those obtained from Inverse Solution 4 for Tests A1, A2, and A3.

Test	Hydraulic Parameters (θ_r = 0.008 $cm^3\ cm^{-3}$)			
	α (cm^{-1})	n (−)	θ_s ($cm^3\ cm^{-3}$)	K_s ($cm\text{-}sec^{-1}$)
A1, IS1	0.05244	6.999	0.463	0.01188
A1, IS2	0.04496	5.762	0.350	0.01135
A1, IS3	0.0445	3.484	0.500	0.01219
A1, IS4	0.04083	5.994	0.282	0.01102
A2, IS1	0.05729	7.000	0.432	0.00960
A2, IS2	0.05020	5.998	0.350	0.00908
A2, IS3	0.0509	3.105	0.482	0.01024
A2, IS4	0.04795	3.015	0.374	0.00920
A3, IS1	0.04351	6.281	0.249	0.00806
A3, IS2	0.03993	4.290	0.350	0.00821
A3, IS3	0.0429	5.826	0.261	0.00808
A3, IS4	0.04470	5.269	0.315	0.00821
B1, IS1	0.0474	4.242	0.205	0.00321
B1, IS2	0.03896	2.124	0.350	0.00356
B1, IS3	0.0434	2.742	0.261	0.00339
B2, IS1	0.04755	7.000	0.221	0.00394
B2, IS2	0.03561	2.568	0.350	0.00418
B2, IS3	0.03895	3.186	0.277	0.00408

TABLE 3 Hydraulic parameter estimates obtained from inverse solutions IS1-IS4 for Set A and Set B tests

Test Method	Hydraulic parameters			
	α (cm^{-1})	n (−)	θ_r ($cm^3\ cm^{-3}$)	θ_s ($cm^3\ cm^{-3}$)
Extraction/Sorption (wetting curve) (Singleton 1997)	0.139	2.17	0.042	0.35
Capillary rise (wetting curve) (Singleton 1997)	0.086	3.60	0.008	0.33
Pressure plate (drying curve) (Singleton 1997)	0.045	1.61	0.008	0.35

TABLE 4 Soil-moisture retention curve paramenters obtained with standard laboratory methods

Test method	Mean K_s value, ($cm\text{-}sec^{-1}$)
Constant head inflow test, cone permeameter (Leonard 1997)	0.0134
Slug tests (Scaturo 1993)	0.00725
Guelph permeameter tests (Singleton 1997)	0.0190
Guelph permeameter tests (Scaturo 1993)	0.00349
Constant head test, laboratory samples (Singleton 1997)	0.00385

TABLE 5 Results of laboratory and in situ tests for saturated hydraulic conductivity

Estimates of the parameters [alpha], *n,* $[\theta]_s$, and K_s obtained solely from the cone permeameter flow responses (Inverse Solution 1) provided the best fit of measured data for all numerical solutions, as expected, because there were no additional constraints (such as moisture contents) on the inverse solution. The resulting retention curves for all tests had the same shape except for pressure heads near zero, where the shapes of the characteristic curves were strongly influenced by the value of $[\theta]_s$. The resulting saturated moisture content, $[\theta]_s$, was also either much higher (Tests A1 or A2), or much smaller (Tests A3, B1, and B2) than that obtained from the laboratory test methods.

Nonuniqueness of $[\theta]_s$ values was anticipated by the results of earlier numerical experiments with error-free synthetic data. Gribb (1996) showed that an objective function similar to Eq. (6) was sensitive to K_s and [alpha] but not sensitive to $[\theta]_s$ and *n.* Because $[\theta]_s$ was not estimated reliably for this test, Inverse Solution 2 was performed to investigate the influence of $[\theta]_s$ on the other parameter estimates. In this case, $[\theta]_s$ was set equal to 0.35 cm^3/cm^3 and parameters [alpha], *n,* and K_s were optimized. The simulated cumulative flow data either underestimated reality slightly when $[\theta]_s$ resulting from Inverse Solution 1 was higher than 0.35 cm^3/cm^3 (Tests A1 and A2) or fit the measured data very well when $[\theta]_s < 0.35$ cm^3/cm^3 (Tests A3, B1 and B2). The underestimation of the cumulative flow volume was a consequence of the simulated low capacity of the soil for imbibition of water. It seems that the real flow regime was influenced by anisotropy and heterogeneities caused by backfilling or the applied Eqs (4) and (5), with $l = 0.5$, are not accurate enough to describe the shapes of both hydraulic properties. As it is beyond the scope of this study, we will concentrate on this problem in our next series of experiments. The modeled pressure heads at the position of the lower tensiometer tracked closely to observed data for all tests. However, the simulated pressure heads at the position of the upper tensiometer showed earlier progressions of the wetting front when compared with the measured data for all tests. Similar to the influence of $[\theta]_s$ on cumulative flow data discussed previously, the course of pressure head changes in time was steeper (if $[\theta]_s$ from Inverse Solution 1 was higher than 0.35 cm^3/cm^3) or more gradual (if $[\theta]_s < 0.35$ cm^3/cm^3) than the observed data. However, the final simulated and observed pressure head responses were almost the same in all cases. Comparison of the soil hydraulic properties resulting from Inverse Solutions 1 and 2 shows that the optimized parameter K_s seems to be correlated to $[\theta]_s$ as well, e.g., K_s is larger/smaller with larger/smaller $[\theta]_s$, whereas [alpha] and *n* are always smaller for Inverse Solution 2 (e.g., the retention curves have more gradual slopes). In addition, the lower the value of $[\theta]_s$ obtained from Inverse Solution 1, the more gradual the retention curve returned from Inverse Solution 2. It must be noted that $[\theta]_r$ can be optimized instead of $[\theta]_s$ with $[\theta]_s$ set equal to a laboratory derived value (0.35 cm^3/cm^3). In cases in which Inverse Solution 1 returned $[\theta]_s$ values less than 0.35, $[\theta]_r$ will be equal to 0.35 - [theta] *IS1* [over] *s* + [theta] *IS1* [over] *r*, (where [theta] *IS1* [over] *s*, [theta] *IS1* [over] *r* are from Inverse Solution 1). The values of [alpha], *n* and K_s, as well as the simulated flow responses, will remain unchanged. The only effect will be a shift of the Inverse Solution 1 [theta](*h*) curve along the [theta] axis. However, this does not improve soil hydraulic property estimates in our examples because the resulting residual moisture content would be too high. For cases with $[\theta]_s$ higher than 0.35 cm^3/cm^3, the resulting $[\theta]_r$ would have the tendency to go to zero and the inversion results would be similar to those of Inverse Solution 2.

For Inverse Solutions 3 and 4, the four parameters [alpha], *n,* $[\theta]_s$ and K_s were estimated. Additional soil moisture data were used in the optimization process to obtain more realistic values of $[\theta]_s$. Initial moisture content data were used for Inverse Solution 3, whereas final moisture content data were added to the objective function for Inverse Solution 4.

The fit of measured data resulting from Inverse Solution 3 is better than for Inverse Solution 2. The cumulative flow volumes were predicted very well, but the simulated tensiometer responses increased more gradually than the measured values for all tests. The fixed point of the retention curve close to residual values resulted in higher values of $[\theta]_s$ and K_s and lower values of [alpha] and *n.* Correlation between $[\theta]_s$ and K_s values, as discussed previously, was again evident. As mentioned before, approximately the same initial moisture contents were observed for different initial tensiometers readings. This is especially curious in the case of Test A3. We expected higher initial moisture contents because the surface of the soil was lightly irrigated overnight before testing, and the initial tensiometer readings were correspondingly higher. It seems for a wetting process of this type, the retention curve follows a shape similar to that determined with the computer-automated extraction/sorption method. The resulting courses of the retention curves show clearly the effect of fixed points of the retention curve, i.e., the influence of the initial conditions that produce different scanning retention curves.

Inverse Solution 4 yielded the worst fit of measured data of all four types of solutions because of constraints imposed by the final moisture content inputs. However, the soil moisture inputs for higher levels of saturation resulted in estimates of $[theta]_s$ similar to values obtained with standard laboratory techniques. Compared with Inverse Solution 1, the hydraulic parameters changed in a manner similar to that of Inverse Solutions 2 and 3. However, there was no correlation among the results from the four different numerical analyses because of different priorities in the objective function and, consequently, the optimization process. In addition, the shapes of the retention curves were influenced strongly by the moisture content values [theta], which were paired with simulated pressure heads, *h.* These [theta] values were determined at different times and at variable positions with respect to the water source for different levels of soil saturation.

Review of the fits of the four inverse solutions for all five tests shows that there is very good coincidence of measured and simulated data for all solutions for Test A3. However, different soil hydraulic properties were obtained from these solutions. Such nonuniqueness is probably caused by the smaller range of pressure head changes detected during this test compared with the other tests.

Comparison of the estimated parameters from the four inverse solutions for each test shows that the values of K_s obtained are almost the same for all numerical analyses. Values of [alpha] are similar for all inverse solutions as well, whereas values of $[theta]_s$ and n vary.

Influence of Applied Pressure Head at the Source and Initial Conditions

The influence of applied pressure heads on the course of the experiment, and, finally, on the optimization results, is possible to see via comparison of tests with similar initial tensiometers readings: Set A, Test A1 (applied pressure head h_0 = 52.5 cm) versus Test A2 (h_0 = 32.5 cm), and Set B, Test B1 (h_0 = 32.5 cm) versus Test B2 (h_0 = 52.5 cm). In both cases, numerical analysis of data from tests with lower applied pressure heads resulted in lower optimized values of $[theta]_s$ and K_s than those estimated from tests run with higher applied pressure heads. For instance, in the case of Inverse Solution 1, the optimized saturated moisture contents, $[theta]_s$, were 0.463 cm^3/cm^3 (Test A1) versus 0.432 cm^3/cm^3 (Test A2) and 0.205 cm^3/cm^3 (Test B1) versus 0.221 cm^3/cm^3 (Test B2). The saturated hydraulic conductivities, K_s, were 0.01188 cm/s (Test A1) versus 0.00960 cm/s (Test A2), and 0.00321 cm/s (Test B1) versus 0.00394 cm/s (Test B2). The effect of applied pressure head on $[theta]_s$ and K_s is evident for all other solutions and other tests (see Table 3) with the exception of Inverse Solution 2 ($[theta]_s$ value fixed and Inverse Solution 4. The results of Inverse Solution 4 were influenced predominantly by the additional soil moisture content data and, as such, the effect of applied pressure head could not be detected. We simulated the courses of Test A2 and B1 with the hydraulic parameters obtained from Inverse Solution 1 for Test A1 and B2, respectively. Only the final pressure heads and total cumulative infiltration volumes are shown in Table 6. The simulated final pressure heads were similar to final readings of the tensiometers (Table 1). On the other hand, the predicted final cumulative infiltration volumes were noticeably lower than the observed volumes (Table 1). We suspect that the lower infiltration capacity indicated from tests with lower applied pressure heads was caused by encapsulated air in the soil or the occurrence of preferential flow, which can be different for different pressure conditions. Investigation of these effects would require continuous measurement of soil moisture and/or pressure heads at different locations in the domain during testing.

Simulated experiment	Source of hydraulic parameter inputs	Final pressure heads (cm)		Final cumulative infiltration volume (cm^3)
		Lower tensiometer	Upper tensiometer	
Test A2	Test A1, IS1	−10.8	−18.3	8071
Test A3	Test A2, IS1	−10.0	−17.8	6395
Test B1	Test B2, IS1	−13.2	−22.7	2469

TABLE 6 Simulated final conditions for Tests A2, A3 and B1

The influence of initial conditions can be examined on examples with the same applied pressure heads (h_0 = 32.5 cm), but with different initial readings of the lower and upper tensiometers, as with Tests A2 and A3 (-47.4 cm and -49.3 cm versus -30.2 cm and -31.5 cm). In the case of higher initial pressure head readings, optimized values of $[\theta]_s$ and K_s were lower than those obtained for tests with lower initial pressure head readings. For Inverse Solution 1, the optimized saturated moisture contents, $[\theta]_s$, were 0.432 cm^3/cm^3 (Test A2) versus 0.249 cm^3/cm^3 (Test A3) and saturated hydraulic conductivities, K_s, were 0.00960 cm/s (Test A2) versus 0.00806 cm/s (Test A3). The effect of initial pressure heads on $[\theta]_s$ and K_s is evident for all solutions (Table 3) with the exception of Inverse Solutions 2 and 4. We simulated the course of Test A3 with hydraulic parameters from Inverse Solution 1 for Test A2 (Table 6). We obtained a higher final cumulative infiltration volume than the observed volume, which indicated lower infiltration capacity as described previously. The flow regime also seemed to be affected by hysteresis of the soil hydraulic properties as the final pressure heads were also overestimated.

An analysis of results for Set A shows a decreasing trend of optimized K_s values with decreasing initial induced hydraulic gradients. In addition, these K_s values are lower than the mean value of K_s (0.0134 cm/s) found from cone permeameter tests performed under saturated conditions (Gribb et al. 1998). As a result, a higher applied pressure head is more likely to yield estimates of K_s closer to those obtained under saturated conditions. On the other hand, a lower applied pressure head is desirable because the rates at which pressure heads increase at the tensiometers are slower, providing more information for more accurate determination of [alpha] and *n.* However, from a practical point of view, the optimized K_s values are not so different from each other, and we believe that the investigated range of 32.5 to 52.5 cm of applied pressure head is suitable for this type of soil. Finally, as already required for uniqueness of the inverse solutions, initial pressure heads in the soil should be as low as possible.

Comparison of Results for Sets A and B and Comparison of the Soil Hydraulic Characteristics Obtained via Inverse Solution and Other Techniques

The results of the two sets of tests presented here are noticeably different. The main influences are likely to be (i) disturbance of soil surrounding the cone (such as densification) caused by pushing or (ii) structural differences between the backfilled and well consolidated soil. It seems that soil structure changes caused by direct push are not dominant for this soil at the investigated depth. The results of both sets are within the range of hydraulic properties obtained with other standard tests performed in situ and in the laboratory on different types of samples. The characters of the retention curves obtained from Inverse Solution 1 for all tests are most similar to the retention curve determined from capillary rise tests conducted on repacked soil columns. For Tests A1 and A2, the first parts of the retention curves are essentially the same for all other solutions despite largely varying $[\theta]_s$ values. The retention curves found for Tests A3, B1, and B2 with $[\theta]_s$ fixed or estimated close to 0.35 cm^3/cm^3 have more gradual shapes and lie between the two limiting branches of the retention curves obtained from capillary rise tests (wetting) and pressure plate tests (drying) performed on undisturbed samples. The shapes of the retention curves close to the limiting or scanning wetting branches of the retention curves were expected because of the wetting character of the experiment and also because $[\theta]_r$ was set equal to 0.008 cm^3/cm^3. In general, the optimized saturated water contents for the pushed cone tests tended to be lower than for the buried cone test.

Saturated hydraulic conductivities obtained for the buried cone permeameter (Set A) are similar to K_s values obtained with the Guelph permeameter (Singleton 1997) and with slug tests (Scaturo 1993), whereas K_s values for the pushed cone permeameter (Set B) are closer to those obtained by Scaturo (1993) with the Guelph permeameter and to laboratory constant head tests (Singleton 1997). On average, the saturated hydraulic conductivity for the buried cone tests were two to three times higher than those for the pushed cone. For most practical applications, such differences would be acceptable. Although it is possible that these decreases (as with $[\theta]_s$) were attributable to lower porosity close to the cone as a result of densification during pushing to the test depth, it must be noted that results tests performed in a consolidated soil profile are influenced highly by soil heterogeneity. Thus natural consolidation, the presence of clay particles, and pseudoaggregation may have influenced the data obtained from the pushed cone permeameter more than that obtained with the buried one.

CONCLUSIONS

We have presented here a modified cone penetrometer tool for simultaneous determination of the soil-moisture characteristic and hydraulic conductivity curves in unsaturated soil. We studied the influence of applied boundary and initial conditions on the final stage and on the estimated values of parameters describing soil hydraulic properties. We found that higher applied pressure head and lower initial pressure head conditions resulted in higher final pressure head readings and, consequently, higher values of $[\theta]_s$ and K_s. We examined the impact of the different sets of optimized parameters and various inputs to the objective function. Logically, the numerical analysis of the cone permeameter flow responses alone provided the best fits of measured data, but values of $[\theta]_s$ were not estimated reliably. On the other hand, restriction of $[\theta]_s$ or improved estimates of $[\theta]_s$ using additional soil moisture content information yielded worse fits of observed data. We see several ways to improve the solution. First, as discussed for the tests when the cumulative flow volumes were underestimated, the effect of anisotropy can be introduced as an additional parameter to be optimized. Secondly, the pore-connectivity parameter, *l,* in Eq. (5) can also be optimized to increase flexibility of the hydraulic conductivity curves, which in this case will probably yield sharper decreases in $K([\theta])$ with decreasing moisture content. For other tests, when $[\theta]_s$ values were too low, the importance of either fixing values of $[\theta]_s$ or $[\theta]_r$ at reasonable values or adding soil moisture content information to find the appropriate position of the retention curve is evident. However, our results in a laboratory aquifer composed of sandy soil showed that the saturated hydraulic conductivity was well estimated. For cases in which the saturated moisture content was estimated or fixed near the laboratory-derived value, the soil-moisture characteristic curves were between the wetting and drying curves obtained from other standard laboratory methods. Differences in the optimized parameter, [alpha], and, to some degree, *n,* within both experimental sets were minimal.

In this study, we analyzed only the wetting part of the cone experiment so that the wetting branches of soil hydraulic properties were obtained. We found that our method predicts values of K_s and [alpha] very well and that the others are reasonably estimated. The soil extraction method of Inoue et al., (1998) is a comparable technique, with a similar flow domain but the reverse flow process used to obtain the drying branches of the soil hydraulic properties. This method was found to be more sensitive to *n* and $[\theta]_r$ but not suitable for prediction of K_s and [alpha] for sandy soils. There is no simple technique other than this method for numerical estimation of drying curves in situ in real time. From inspection of the wetting and redistribution phases of cone permeameter tests (see Gribb et al. (1998)), it seems that it should be possible to obtain estimates of the both the wetting and drying curves. This will be our next subject of study.

It is well known that the soil fabric is disturbed as a result of cone placement; however, the results of these few tests in sandy soil show little impact of disturbance on the values of K_s or [alpha], *n,* and $[\theta]_s$ returned from the optimization procedure. It is likely that disturbance effects will be more significant in other soil types. This will be also studied further in the field.

ACKNOWLEDGMENTS

The authors acknowledge M. F. Leonard for performing the cone tests in the laboratory aquifer and S. C. Anderson and J. E. Singleton for performing the other laboratory tests. Support of this work by the U.S. Army Research Office, grant DAAH04-95-1-0228, and the National Science Foundation, CAREER grant CMS-9501772, is gratefully acknowledged. The authors also thank the anonymous reviewers for their helpful comments and suggestions.

REFERENCES

ASTM. 1994. Standard test method for capillary-moisture relationships for coarse-and medium-textured soils by porous-plate method, D-2325, vol. 4.08. Soil and rock, dimension stone, geosynthetics. ASTM, Philadelphia, PA.

ASTM. 1993. Standard test method for permeability of granular soils (constant head), D-2334, vol. 4.08. Soil and rock, dimension stone, geosynthetics. ASTM, Philadelphia, PA.

Bard, Y. 1974. Nonlinear parameter estimation. Academic Press, New York. [Context Link]

Benson, C.H., and M.M. Gribb. 1997. Measuring unsaturated hydraulic conductivity in the laboratory and field. Unsaturated soil engineering practice. Geotech. Spec. Publ. No. 68, S. L. Houston and D. G. Fredlund, eds. ASCE, New York, NY, pp. 113-168. [Context Link]

Bohne, K., C. Roth, F. J. Leij, and M. Th. van Genuchten. 1993. Rapid method for estimating the unsaturated hydraulic conductivity from infiltration measurement, Soil Sci. 155:237-244. [Context Link]

Bouwer, H., and R. C. Rice. 1976. A slug test for determining hydraulic conductivity of unconfined aquifers with completely or partially penetrating wells, Water Resour. Res. 12:423-428. [Context Link]

Carrera, J., and S. P. Neuman. 1986. Estimation of aquifer parameters under transient and steady state conditions. 2. Uniqueness, stability, and solution algorithms. Water Resour. Res. 22:211-227. [Context Link]

Ciollaro, G., and N. Romano. 1995. Spatial variability of the soil hydraulic properties of a volcanic soil. Geoderma 65:263-282. [Context Link]

Eching, S. O., and J. W. Hopmans. 1993. Optimization of hydraulic functions from transient outflow and soil water pressure data. Soil Sci. Soc. Am. J. 57:1167-1175. [Context Link]

Eching, S.O., J. W. Hopmans, and O. Wendroth. 1994. Unsaturated hydraulic conductivity from transient multi-step outflow and soil water pressure data. Soil Sci. Soc. Am. J. 58:687-695. [Context Link]

Gribb, M. M. 1996. Parameter estimation for determining hydraulic properties of a fine sand from transient flow measurements. Water Resour. Res. 32:1965-1974. [Context Link]

Gribb, M. M. 1993. At depth determination of hydraulic conductivity of unsaturated porous media via analysis of transient flow data. Ph.D. dissertation, University of Wisconsin-Milwaukee, WI. [Context Link]

Gribb, M.M.,J. Šimunek, and M. F. Leonard. 1998. Use of a cone penetrometer method to determine soil hydraulic properties. J. Geotech and Geoenviron. Engr. (*in press*). [Context Link]

Hvorslev, M.J. 1951. Time lag and soil permeability in ground-water observations. WES Bulletin No. 36. US Army Corps of engineers, Vicksburg, MS. [Context Link]

Inoue, M., J. Šimunek, J. W. Hopmans, and V. Clausnitzer. 1998. In-situ estimation of soil hydraulic functions using a multi-step soil-water extraction technique. Water Resour. Res. (*in press*). [Context Link]

Klute, A., and C. Dirksen. 1986. Hydraulic conductivity and diffusivity: Laboratory methods. *In* Methods of soil analysis, part 1. Physical and mineralogical methods, 2nd Ed. A. Klute (ed.). SSSA, Madison, WI, pp. 687-729. [Context Link]

Kool, J. B., J. C. Parker, and M. Th. Van Genuchten. 1987. Parameter estimation for unsaturated flow and transport models-A review. J. Hydrol. 91: 255-293. [Context Link]

Kool, J. B., J. C. Parker, and M. Th van Genuchten. 1985. Determining soil hydraulic properties from one step outflow experiments by parameter estimation: I. Theory and numerical studies. Soils Sci. Soc. Am. J. 49:1348-1354. [Context Link]

Lambe, W. T. 1951. Capillary phenomena in cohesionless soils. Trans. ASCE 116:401-423. [Context Link]

Leonard, M. F. 1997. Design and laboratory evaluation of a cone permeameter for unsaturated soil hydraulic parameter determination. MS thesis, Univ. of South Carolina, Columbia, SC. [Context Link]

Marquardt, D. W. 1963. An algorithm for least-squares estimation of non-linear parameters. J. Ind. Appl. Math. 11:431-441. [Context Link]

Mualem, Y. 1976. A new model for predicting the hydraulic conductivity of unsaturated porous media. Water Resour. Res. 12:513-522. [Context Link]

Parker, J. C., J. B. Kool, and M. Th. van Genuchten. 1985. Determining soil properties from one-step outflow experiments by parameter estimation, II. Experimental studies. Soil Sci. Soc. Am. J. 49:1354-1359. [Context Link]

Ray, R. P., and K. B. Morris. 1994. Automated laboratory testing for soil/water characteristic curves. Proc. 1st Internatl Conf. Unsaturated Soils. E. Alonso and P. Delage (eds.). Balkema, Rotterdam, The Netherlands, pp. 236-241. [Context Link]

Reynolds, W. D. 1993. Unsaturated hydraulic conductivity: Field measurement. *In* Soil sampling and methods of analysis. M. R. Carter, (ed.). Can. Soc. Soil Sci., Lewis Publishers, Boca Raton, FL, pp. 633-644. [Context Link]

Richards, L. A. 1931. Capillary conduction of liquids through porous mediums. Physics 1:318-333. [Context Link]

Russo, D., E. Bresler, U. Shani, and J. C. Parker. 1991. Analyses of infiltration events in relation to determining soil hydraulic properties by inverse-problems methodology. Water Resour. Res. 27:1361-1373. [Context Link]

Santini, A., N. Romano, G. Ciollaro, and V. Comegna. 1995. Evaluation of a laboratory inverse method for determining unsaturated hydraulic properties of a soil under different tillage practices, Soil Sci. 160:340-351. [Context Link]

Scaturo, D. M. 1993. Evaluation of multi-level direct push sampling for hydraulic conductivity analysis. MS thesis, Univ. of South Carolina, Columbia, SC. [Context Link]

Šimunek, J., M. Šejna, and M. Th. van Genuchten. 1996. HYDRUS-2D, Simulation water flow and solute transport in two-dimensional variably saturated media, Version 1.0, IGWMC-TPS-53. International Groundwater Modeling Center, Colo. School of Mines, Golden, CO. [Context Link]

Šimunek, J., O. Wendroth, and M. Th. van Genuchten. 1998a. A parameter estimation analysis of the evaporation method for determining soil hydraulic properties. Soil Sci. Soc. Am. J. (*in press*). [Context Link]

Šimunek, J., M. Th. van Genuchten, M. M. Gribb, and J. W. Hopmans. 1998b. Parameter estimation of soil hydraulic properties from transient flow processes, Soil Tillage Res. (*in press*). [Context Link]

Šimunek, J., and M. Th. van Genuchten. 1997. Estimating unsaturated soil parameters from multiple tension disc infiltrometer data. Soil Sci. 162:383-398. Ovid Full Text | [Context Link]

Šimunek, J., and M. Th. van Genuchten. 1996. Estimating unsaturated soil hydraulic properties from tension disk infiltrometer data by numerical inversion. Water Resour. Res. 32:2683-2696. [Context Link]

Singleton, J.E. 1997. Hydraulic characteristics of a laboratory aquifer. MS thesis, Univ. of South Carolina, Columbia, SC. [Context Link]

Toorman, A. F., P. J. Wierenga, and R. G. Hills. 1992. Parameter estimation of hydraulic properties from one-step outflow data. Water Resour. Res. 28:3021-3028. [Context Link]

van Dam, J. C., N. M. Stricker, and P. Droogers. 1992. Inverse method for determining soil hydraulic functions from one-step outflow experiments. Soil Sci. Soc. Am. J. 56:1042-1050. [Context Link]

van Dam, J. C., N. M. Stricker, and P. Droogers. 1994. Inverse method to determine soil hydraulic functions from multi-step outflow experiments. Soil Sci. Soc. Am. J. 58:647-652. [Context Link]

van Genuchten, M. Th., F.J. Leij, and S. R. Yates. 1991. The RETC code for quantifying the hydraulic functions of unsaturated soils. US EPA, Ada, OK. [Context Link]

van Genuchten, M. Th. 1980. A closed-form equation for predicting the hydraulic conductivity of unsaturated soils. Soil Sci. Soc. Am. J. 44:892-898. [Context Link]

Wind, G. P. 1968. Capillary conductivity data estimated by a simple method. *In* Water in the unsaturated zone. P.E. Rijtema and H. Wassink (eds.). Proc. Wageningen Symp., IASAH, Gentbrugge, pp. 181-191. [Context Link]

Key words: Soil hydraulic properties; parameter estimation; cone penetration testing; unsaturated hydraulic conductivity; inverse modeling

---

IMAGE GALLERY

Select All

Export Selected to PowerPoint

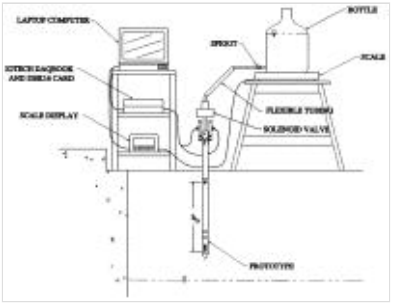

Fig. 1

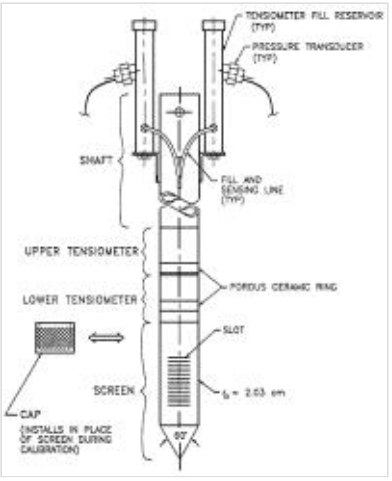

Fig. 2

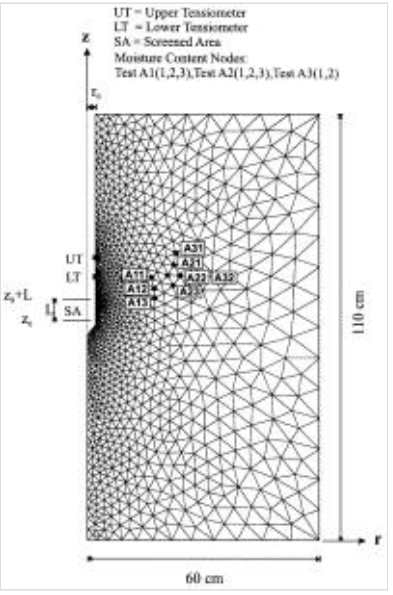

Fig. 3

$$\frac{1}{r}\frac{\partial}{\partial r}\left[r\,K\frac{\partial h}{\partial r}\right]+\frac{\partial}{\partial z}\left[K\left(\frac{\partial h}{\partial z}+1\right)\right]=\frac{\partial\theta}{\partial t}$$

Equation 1

$$h\,(r,z,t)=h_i\,(r,z)\qquad t=0$$

Equation 2

$$h\,(r,z,t)=h_o-(z-z_o)\quad r=r_o,\ z_o<z<z_o+L$$

Equation 3

$$\theta_e=\frac{\theta(h)-\theta_r}{\theta_s-\theta_r}=\frac{1}{(1+|\alpha h|^n)^m}\quad h<0$$

$$\theta_e=1,\ h\geq 0$$

Equation 4

$$K(\theta)=K_s\,\theta_e^{l}\left[1-(1-\theta_e^{1/m})^m\right]^2\quad h<0$$

$$K\,(\theta)=K_s\quad h\geq 0$$

Equation 5

$$\Phi(b,q,p)=\sum_{j=1}^{n_q}\nu_j\sum_{i=1}^{N_q}w_{i,j}\left[q_j^*(x,t)-q_j(x,t,b)\right]^2+\sum_{j=1}^{n_p}\nu_j\sum_{i=1}^{N_p}w_{i,j}\left[p_j^*(\theta_i)-p_j(\theta_i,b)\right]^2+\sum_{j=1}^{n_b}\nu_j\left[b_j^*-b_j\right]^2$$

Equation 6

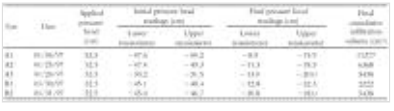

Table 1

Table 2

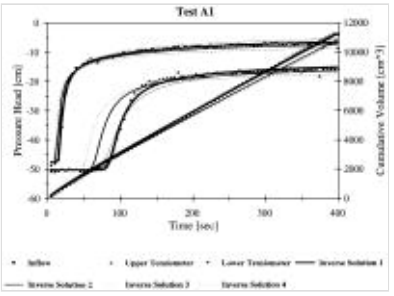

Fig. 4

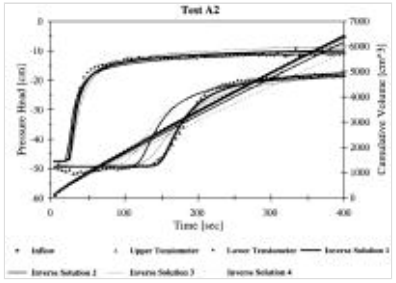

Fig. 5

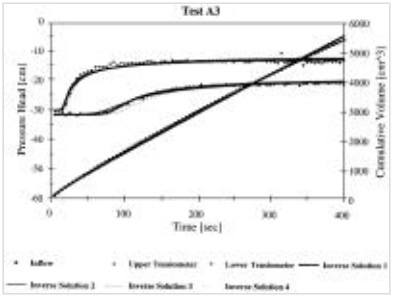

Fig. 6

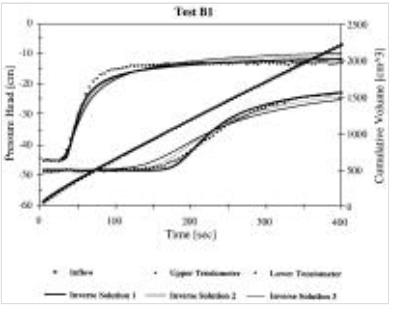

Fig. 7

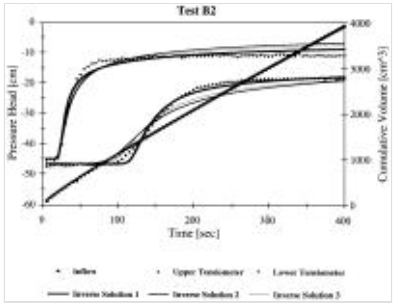

Fig. 8

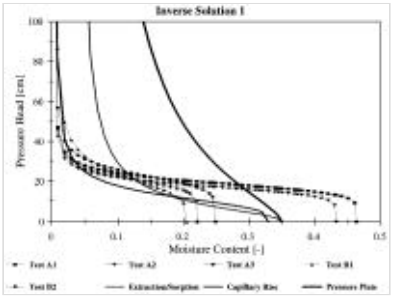

Fig. 9

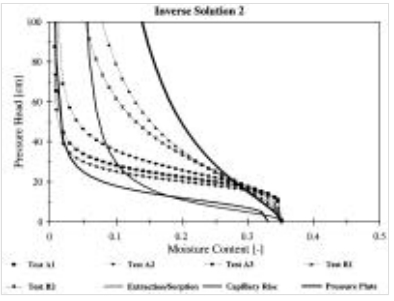

Fig. 10

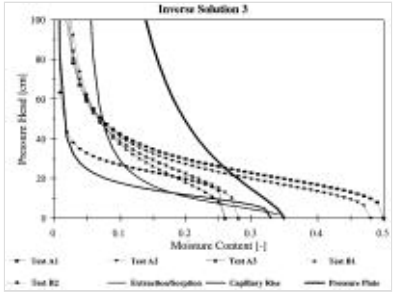

Fig. 11

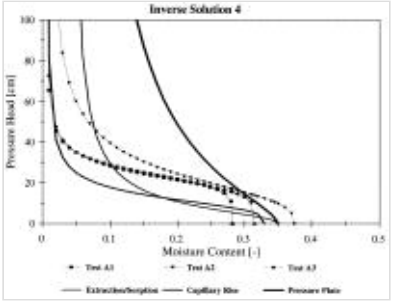

Fig. 12

Test	Hydraulic Parameters (θ_r = 0.008 cm^3 cm^{-3})			
	α (cm^{-1})	n (–)	θ_s (cm^3 cm^{-3})	K_s (cm-sec^{-1})
A1, IS1	0.05244	6.999	0.463	0.01188
A1, IS2	0.04496	5.762	0.350	0.01135
A1, IS3	0.0445	3.484	0.500	0.01219
A1, IS4	0.04083	5.994	0.282	0.01102
A2, IS1	0.05729	7.000	0.432	0.00960
A2, IS2	0.05020	5.998	0.350	0.00908
A2, IS3	0.0509	3.105	0.482	0.01024
A2, IS4	0.04795	3.015	0.374	0.00920
A3, IS1	0.04351	6.281	0.249	0.00806
A3, IS2	0.03993	4.290	0.350	0.00821
A3, IS3	0.0429	5.826	0.261	0.00808
A3, IS4	0.04470	5.269	0.315	0.00821
B1, IS1	0.0474	4.242	0.205	0.00321
B1, IS2	0.03896	2.124	0.350	0.00356
B1, IS3	0.0434	2.742	0.261	0.00339
B2, IS1	0.04755	7.000	0.221	0.00394
B2, IS2	0.03561	2.568	0.350	0.00418
B2, IS3	0.03895	3.186	0.277	0.00408

Table 3

Test Method	Hydraulic parameters			
	α (cm^{-1})	n (–)	θ_s (cm^3 cm^{-3})	θ_r (cm^3 cm^{-3})
Extraction/Sorption (wetting curve) (Singleton 1997)	0.139	2.17	0.042	0.35
Capillary rise (wetting curve) (Singleton 1997)	0.086	3.60	0.008	0.33
Pressure plate (drying curve) (Singleton 1997)	0.045	1.61	0.008	0.35

Table 4

Test method	Mean K_s value, (cm-sec^{-1})
Constant head inflow test, cone permeameter (Leonard 1997)	0.0134
Slug tests (Scatuzo 1993)	0.00725
Guelph permeameter tests (Singleton 1997)	0.0190
Guelph permeameter tests (Scatuzo 1993)	0.00349
Constant head test, laboratory samples (Singleton 1997)	0.00385

Table 5

Table 6

Back to Top